ISBN: 978-3-95450-232-5 ISSN: 2673-7000 doi:10.18429/JACoW-NAPAC2022-TUPA74

NUMERICAL CALCULATIONS OF WAVE GENERATION FROM A BUNCHED ELECTRON BEAM IN SPACE*

H. Xu†, L. D. Duffy, Q. R. Marksteiner, G. D. Reeves, G. L. Delzanno,
Los Alamos National Laboratory, Los Alamos, NM, USA

Abstract

We present our numerical approach and preliminary results of the calculations of whistler and X mode wave generation by a bunched electron beam in space. The artificial generation of whistler and X mode plasma waves in space is among the candidate techniques to accomplish the radiation belt remediation (RBR), in an effort to precipitate energetic electrons towards the atmosphere to reduce their threat to low-Earth orbit satellites. Free-space propagation of an electron pulse in a constant background magnetic field was simulated with the CST particle-in-cell (PIC) solver, with the temporal evolution of the beam recorded. The SpectralPlasmaSolver (SPS) was then modified to use the recorded electron pulse propagation to calculate the real-time plasma waves generated by the beam. SPS simulation results of the wave generation for the upcoming Beam-PIE experiment as well as an idealized bunched electron beam are shown.

INTRODUCTION

Energetic electrons at MeV level trapped inside the radiation-belt are known to cause damage to the electronics in low-Earth orbit satellites [1]. Theoretical calculations have shown that artificially generated plasma waves in space, e. g. the whistler and the X mode waves, are capable of precipitate these energetic electrons towards the atmosphere, accomplishing the Radiation-Belt Remediation (RBR). The plasma waves in space can be generated by antennas or by electron beams. This paper addresses the preliminary theoretical investigation of space plasma wave generation by an electron beam produced by an space-borne accelerator.

The simulations of plasma wave generation by a pulsed electron beam are performed using the SpectralPlasmaSolver (SPS) code [2], a high performance 3D fluid-kinetic numerical solver of Vlasov-Maxwell equations. The original version of SPS uses analytical expression of the current densities for the calculations of plasma wave generation, with which the initial simulations of the wave generation in the whistler and the X mode were carried out [3]. In order to study the plasma wave generation in a more realistic scenario, the SPS code was later modified to take the numerical description of the electron beam current density spatial distribution variation in time over the course of the beam propagation in a background magnetic field as the input, which was calculated by the CST [4] particle-in-cell (PIC) solver beforehand, to perform simulations of the real-time generation of plasma waves during the travel of the beam.

Two types of the pulsed electron beams have been investigated in the wave generation simulations. The first type is an example electron beam from the theoretical calculations of the upcoming Beam-PIE experiment [5, 6], at 22.6 keV beam energy, with 13.9 nC total charge, and with an initial total beam pulse length of 2.45 µs. The second type is an idealized bunched beam of 10.0 nC with a much shorter initial pulse total length of 0.10 µs and with 15.0 keV beam energy.

The frequency range of the simulations of the plasma wave generation is from direct current (DC) to the upper hybrid resonance. In this frequency range, the generation of the whistler and the X mode waves is calculated. The power generation spectra are calculated using the surface integral of the Poynting vector over a transverse envelope surrounding the electron beam.

CST PIC SIMULATIONS

The input to the CST PIC solver is a prepared beam file of macroparticles, representing the electron beam as produced by the space-borne accelerator. In the CST PIC simulations, the free space drift of the electron beam along the background magnetic field is calculated. Meanwhile, the 3D position monitor is used to take the snap shots of the spatial charge distribution variation in time, saving the information of all the macroparticles at a constant time interval in the simulation.

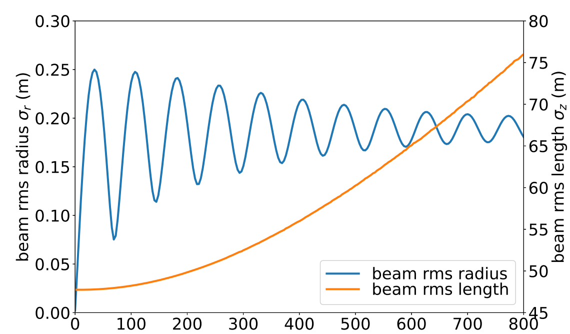

Figure 1: Evolution of the rms radius and the rms beam length of the simulated pulsed electron beam generated by the Beam-PIE experiment as it propagates parallel to the background magnetic field.

As an example, Fig. 1 shows the CST PIC results of the evolution of the simulated Beam-PIE experimental electron beam rms radius and rms beam length versus the distance of propagation of the electron beam parallel with the mag-

* Work supported by the Laboratory Directed Research and Development program of Los Alamos National Laboratory.
† haoranxu@lanl.gov

ISBN: 978-3-95450-232-5 ISSN: 2673-7000 doi:10.18429/JACoW-NAPAC2022-TUPA74

netic field. The oscillation of the beam radius is driven by the transverse space charge force, and the increase of the beam length is due to the longitudinal space charge force as well as the energy spread. As the beam length increases during the propagation, the reduced transverse space charge effect causes the rms beam radius oscillation amplitude to decrease.

It was then confirmed that the oscillation of the transverse beam size, on the scale of that observed in the CST PIC simulations, had little effect on the power spectrum of the plasma wave generation. As a result, SPS uses only the longitudinal electron beam current density temporal evolution from the CST PIC 3D position monitor results; the transverse beam profile is assumed to be Gaussian, with the constant rms transverse size throughout the beam and over the entire propagation duration.

SPS FIELD STRUCTURE

The SPS simulations assume a background magnetic field of $B_0 = 4.53 \times 10^{-5}$ T, and the electron cyclotron frequency is defined as $\omega_{ce} = eB_0/m_e$ (1.27 MHz). The simulation domain is filled with homogeneous plasma, the electron plasma frequency of which is measured $\omega_{pe}/\omega_{ce} = 2$. The cold plasma upper hybrid frequency is then described by $\omega_{uh}/\omega_{ce} = 2.24$. In SPS simulations, linear spatial dimensions are normalized with the electron inertial length $d_e = c/\omega_{pe}$ =18.82 m.

Beam-PIE electron beam

The plasma wave field structure of B_y/B_0 formed on the $\hat{y}$-O-$\hat{z}$ plane after the Beam-PIE experimental beam propagates 504.5 m from z =12.0 d_e to 38.8 d_e along the magnetic field is illustrated in Fig. 2. In the figure, the beam is centered at $x = 0$ and y =14.5 d_e, with the length of the beam spans between z =22.6 d_e and z =46.5 d_e.

Two modes of the plasma wave radiation are visible. The whistler mode is marked by the comparatively longer wave length, on the outer region away from the beam. The X mode field distribution is seen in the inner region with smaller wavelength.

The X mode in the figure is most prominent between z =15 d_e and 20 d_e; the magnitude of X mode declines at a greater z-position, because the electron beam lengthens as it propagates, and the X mode radiation gradually loses coherence. In addition, the thin stripes seen on the entire y-range over z =5 d_e to 20 d_e are not real field pattern, but numerical noise.

Idealized bunched beam

The plasma wave B_y/B_0 field pattern generated by the idealized bunched beam is shown in Fig. 3 on the $\hat{y}$-O-$\hat{z}$ plane, as the electron bunch propagates 362.1 m from z =4.0 d_e to 23.2 d_e.

In general, the radiation coherence is enhanced in the case of the idealized bunched beam with a much shorter initial beam length. In Fig. 3, both the whistler mode in the outer region and the X mode trailing behind the electron beam in the inner region are clearly seen.

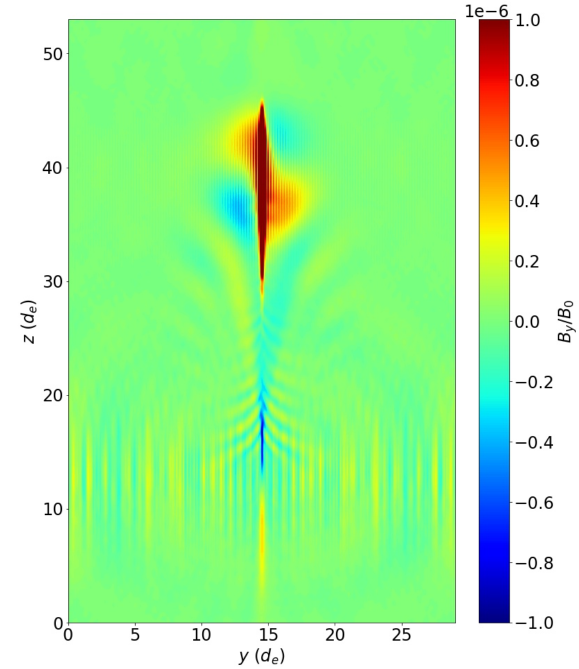

Figure 2: The field pattern of the plasma wave generated by the Beam-PIE electron beam at a propagation distance of 504.5 m, represented by the distribution of B_y/B_0. The beam shown spans from z =22.6 d_e to z =46.5 d_e.

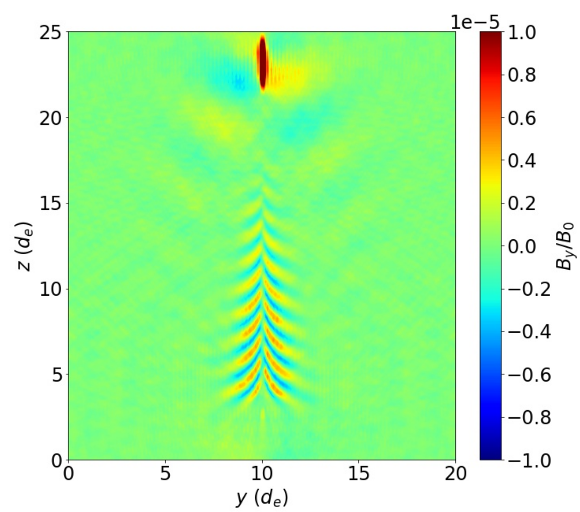

Figure 3: The field pattern of the plasma wave generated by the idealized bunched electron beam at a propagation distance of 362.1 m, represented by the distribution of B_y/B_0. The beam shown spans from z =21.3 d_e to z =25.0 d_e.

ISBN: 978-3-95450-232-5 ISSN: 2673-7000 doi:10.18429/JACoW-NAPAC2022-TUPA74

It is worth noting that, in the case of the idealized bunched beam, the magnitude of the X mode radiation is much greater than that of the whistler mode, indicating potential comparatively more intense interaction by the X mode fields with the energetic electrons in the radiation belt.

SPS SPECTRUM COMPARISON

The radiation spectra of the plasma waves generated from a single electron bunch are calculated for the case of the Beam-PIE electron beam and of the idealized bunched beam. In order to show the power conversion efficiency from the electron beam kinetic energy to the plasma wave radiation, the comparison of the power spectra normalized by the beam charge is given in Fig. 4, where normalized notations are used [3]: $\Omega = \omega/\omega_{ce}$, $\overline{q_b} = q_b/en_0d_e^3$, $\overline{P} = P/en_0c^2d_e^3B_0$. n_0 is the background plasma density.

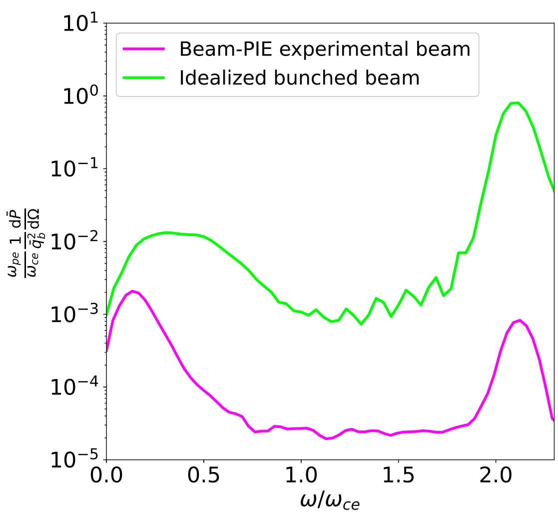

Figure 4: Spectra of the plasma wave radiation by a single electron bunch in the case of the Beam-PIE electron beam (magenta) and of the idealized bunched beam (lime), normalized by the beam charge, plotted versus the normalized frequency $\Omega = \omega/\omega_{ce}$.

The whistler mode radiation has the frequency range of $\omega \leq \omega_{ce}$, while the X mode distribution is on $\omega \geq \omega_{ce}$. In Fig. 4, the peaks on the spectra marking the whistler as well as the X mode radiation are evidently seen. For the whistler mode, the peak of the spectrum magnitude per unit charge for the idealized bunched electron beam case is 9 dB above the case of the Beam-PIE beam; for the X mode, the magnitude peak difference is greater, at 30 dB.

SPS result analysis shows that over the electron beam propagation illustrated in Fig. 2, the Beam-PIE electron beam radiates with an average power of 1.8 mW, releasing 11 nJ total radiation energy, accounting for a portion of 3.4×10^{-5} in the total energy of the beam received from the accelerator. In the case of the idealized bunched beam (Fig. 3), the average radiation power is 0.20 W, and the total radiation energy is 1.0 µJ, which is 0.68% of the electron bunch initial total energy.

The reason for the higher efficiency of plasma wave radiation by the idealized bunched beam is the shorter initial beam length, which results in the greater coherence of radiation. In Fig. 4, the reason for the more prominent enhancement in the peak magnitude difference of the X mode than that of the whistler mode by the idealized bunched beam is that the X mode radiation, due to the shorter wavelength, is more sensitive to the electron beam length.

It is worth further exploring if the X mode waves generated by a much shorter pulsed electron beam in space can be a more efficient approach of accomplishing RBR.

CONCLUSIONS

A theoretical calculation approach has been established using the CST PIC solver and the modified SPS code to perform simulations of the plasma wave generation by a pulsed electron beam in space.

The wave generation using two different types of the electron beams, the Beam-PIE experimental beam and an idealized bunched beam, has been calculated. Both the whistler and the X mode waves are identified on the radiation field structures.

The plasma wave spectrum has been calculated using the SPS simulation results for both the case of the Beam-PIE electron beam and the case of the idealized bunched beam. The characteristic spectrum magnitude peaks of the whistler and the X mode are distinctly identified on the spectrum from each case of the beam simulated. Due to the shorter initial beam length, the idealized bunched beam has overall higher radiation efficiency, with more pronounced enhancement of the X mode radiation efficiency.

REFERENCES

[1] B. E. Carlsten, *et al.*, "Radiation-belt remediation using space-based antennas and electron beams," *IEEE Trans. Plasma Sci.*, vol. 47, no. 5, pp. 2045–2063, 2019. doi:10.1109/TPS.2019.2910829

[2] G. L. Delzanno, "Multi-dimensional, fully-implicit, spectral method for the Vlasov–Maxwell equations with exact conservation laws in discrete form," *J. Comput. Phys.*, vol. 301, no. 15, pp. 338–356, 2015. doi:10.1016/j.jcp.2015.07.028

[3] G. L. Delzanno and V. Roytershteyn, "High-frequency plasma waves and pitch angle scattering induced by pulsed electron beams," *J. Geophys. Res. Space Phys.*, vol. 124, no. 9, 2019. doi:10.1029/2019JA027046

[4] CST Studio Suite, https://www.3ds.com/products-services/simulia/products/cst-studio-suite/

[5] G. D. Reeves, *et al.*, "The beam plasma interactions experiment: An active experiment using pulsed electron beams," *Front. Astron. Space Sci.*, vol. 7, no. 23, 2020. doi:10.3389/fspas.2020.00023

[6] R. D. Reeves, "Electron beams for radiation belt remediation-25527," *Topical Meeting of the Radiation Protection and Shielding Division of ANS*, Santa Fe, NM, USA, 2018.